Rahbar, N., *et al.*: Numerical Investigation on Flow Behavior and Energy …
THERMAL SCIENCE, Year 2015, Vol. 19, No. 2, pp. 619-630

619

NUMERICAL INVESTIGATION ON FLOW BEHAVIOR AND ENERGY SEPARATION IN A MICRO-SCALE VORTEX TUBE

by

Nader RAHBAR[a], Mohsen TAHERIAN[a], Mostafa SHATERI[a], and Mohammad Sadegh VALIPOUR[b]*

[a] Department of Mechanical Engineering, Semnan Branch, Islamic Azad University, Semnan, Iran
[b] School of Mechanical Engineering, Semnan University, Semnan, Iran

There are a few experimental and numerical studies on the behavior of micro-scale vortex tubes. The intention of this work is to investigate the energy separation phenomenon in a micro-scale vortex tube by using the computational fluid dynamic. The flow is assumed as steady, turbulent, compressible ideal gas, and the shear-stress transport k-ω is used for modeling of turbulence phenomenon. The results show that 3-D computational fluid dynamic simulation is more accurate than 2-D axisymmetric one. Moreover, optimum cold-mass ratios to maximize the refrigeration-power and isentropic-efficiency are evaluated. The results of static temperature, velocity magnitude, and pressure distributions show that the temperature-separation in the micro-scale vortex tube is a function of kinetic--energy variation and air-expansion in the radial direction.

Key words: *Ranque-Hilsch tube, micro-scale vortex tube, computational fluid dynamic modeling, energy separation, temperature separation, shear-stress transport turbulence model*

Introduction

Vortex tube or Ranque-Hilsch vortex tube (RHVT) was first discovered by a French physicist Ranque and was granted by him as a patent in 1934 [1, 2]. After that Hilsch [3], a German engineer reported some other characteristics of vortex tubes based on his theoretical and experimental studies. Vortex tubes have no moving parts, compact in size, and their construction is easier than other refrigeration systems. They consist of an entrance block of nozzles, an orifice plate, an adjusting cone-shape valve and inlet and outlet exits. The main remarkable feature of RHVT is their ability to separate cold and hot streams from a source of high-pressure inlet gas. When a high-pressure gas tangentially enters the vortex tube through one or more inlet nozzles, its expansion creates a rapidly spinning vortex. The spinning gas goes through the pipe, some portion of its leave the tube at hot outlet, and the other forced back along the central axis by adjusting valve. Compare to inlet stream, the periphery of the tube has a high temperature, and the central portion has a low temperature. This phenomenon is known as temperature separation in the vortex tubes. Vortex tubes are classified into two types: counter-flow and uni-flow tubes. If the hot and cold exits are located at the same side, the vortex tube is called uni-flow; otherwise, it is a counter-flow vortex tube. Commercially,

___

* Corresponding author; e-mail: nrahbar@gmail.com; rahbar@semnaniau.ac.ir

620

Rahbar, N., *et al.*: Numerical Investigation on Flow Behavior and Energy …
THERMAL SCIENCE, Year 2015, Vol. 19, No. 2, pp. 619-630

there are some applications for vortex tubes: cooling electronic devices, dehumidifying gas samples, cooling parts of machines, and setting solders [4].

Because of their special characteristics, vortex tubes have been an attractive subject for many scientists and researchers. So many experimental and numerical studies have been done to increase the performance or to better understanding of thermal separation in the vortex tubes. In an experimental study, Saidi and Valipour [5] concluded that the effective parameters of a vortex tube are divided into two different types: geometrical and thermophysical properties. They reported that the cold temperature and efficiency decreases when the number of inlet nozzles increases. In addition, the inlet pressure has a direct effect on the cold air temperature difference; meanwhile, there is an optimum-efficiency at a specific inlet pressure. Gao *et al.* [6] conducted some experiments to understand the cooling mechanism, also the pressure, temperature, and velocity distributions inside the vortex tubes. They found that rounding off the entrance can improve the performance of a vortex tubes. They also reported the existence of a secondary circulation inside the tube. In an experimental research, Aydin and Baki [7] reported that inlet pressure and cold fraction are the important parameters influencing the performance of the RHVT. These results were also reported in another study by Hamdan *et al.* [8]. Wu *et al.* [9] modified inlet nozzles and air passage of a RHVT and experimentally showed that these modifications could remarkably improve the performance of a vortex tube. In another study, Nimbalkar and Muller [10] used energy separation and energy flux separation efficiencies to investigate the characteristic of a vortex tube. They reported that the maximum value of energy separation was always happened at a 60% cold fraction irrespective of orifice diameter and inlet pressure. Valipour and Niazi [11] investigated the influence of main tube uniform curvature on the performance of a vortex tube. They reported that these effects depend on inlet pressure and cold mass ratio.

Because of the complex nature of energy separation, it is extremely difficult and expensive to construct an experimental set-up for detailed investigation of the energy separation in vortex tubes. Many researchers tried to use computational fluid dynamics (CFD) to study the separation phenomenon in RHVT. Frohlingsdorf and Unger [12] used a 2-D axisymmetric model to simulate the compressible flow and energy separation with CFX flow solver. They reported that the application of k-ε model leads to substantial differences between measured and calculated tangential velocity profiles. They suggested that, for the calculation of turbulent viscosity, it is possible to replace k-ε model by the correlation from Keyes [13]. Behera *et al.* [14] used STAR-CD commercial code to study the flow behavior in a RHVT. They used RNG k-ε turbulence model to evaluate the velocity components, flow patterns and the optimum parameters of the vortex tube. Aljuwayhel *et al.* [15] used Fluent CFD solver to study the flow behavior within a counter-flow vortex tube. They showed that a work transfer due to the viscous-shear between hot and cold streams is the main reason for unique behavior of vortex tubes. They also reported that the choice of turbulence model has a large effect on estimating of the vortex tube's performance. Skye *et al.* [16] compared the results of RNG k-ε and standard k-ε turbulence models with the results of experimental measurements. They used a 2-D steady axisymmetric model and reported that the standard k-ε (with swirl) has a better prediction of the flow behavior. Eiamsa and Promvonge [4, 17] showed that the results of algebraic stress model (ASM) has a better agreement with experimental data than Standard k-ε model. Ameri and Behnia [18] used 2-D and 3-D RSM turbulence models to investigate the energy separation in a vortex tube. They find an optimum inlet-pressure for maximum efficiency. They also suggested the optimum dimensional values for their vortex tube. Farouk *et al.* [19, 20] used large eddy simulation (LES) technique to predict the gas flow, temperature

fields and species mass fractions in a vortex tube. They showed that axial and azimuthal velocities are dominant parameters. They also reported that cold mass fraction was varied by varying hot exit pressure. Hossein-Nezhad and Shamsoddini [21] compared 2-D and 3-D numerical modeling of the flow stream in a vortex tube. They concluded that the results of a 3-D model, are more accurate than 2-D one. Moreover, in another study [22] they reported that when the number of nozzles is increased, the power of cooling increases and the cold outlet-temperature decreases. Dutta *et al.* [23] compared several different turbulence models and concluded that the results of standard *k-ε* model are the closest to the experimental results.

Most of previous experimental and numerical studies have been conducted on the fairly large tube diameters (*i. e.* 10-25 mm) [24]. A micro-scale vortex tube (MVT) has a good potential for small-scale cooling applications such as cooling of the electronic chips. To the best knowledge of the authors of the present paper, there are not enough investigations on the field of micro-scale vortex tubes. Dyskin and Kramarenko [25] were the first researchers that conducted some experimental procedures to determine the performance characteristics of a micro-scale vortex tube. Their tube had an operating pressure ratio of 6 and diameters of 1 mm, 2 mm, and 3 mm. They reported that, by decreasing of flow-rate, the cooling effect decreases. Hamoudi *et al.* [26] experimentally investigated the separation performance of a micro-scale vortex tube. They conducted some experiments over a wide range of working pressure, different cold air mass ratio, different tube length, and orifice diameters. The results of their experiments at low Reynolds numbers showed that when the Reynolds number increases, the dimensionless temperature increases. They also concluded that, at high inlet pressure, the optimum cold air mass fraction is not constant, and it is higher than the conventional vortex tubes. However, the effect of *L/D* and D_c/D ratios are similar to those in the conventional devices.

As mentioned before, there are few works on the investigation of flow characteristics in micro-scale vortex tubes. The aim of the present work is to investigate the energy separation phenomenon in a typical micro-scale vortex tube by using of computational fluid dynamic. In addition, distributions of the pressure, static temperature and velocity components are obtained to study the flow characteristics in the micro-scale vortex tube.

Numerical model formulation

In this study, the numerical analysis of fluid regime in a micro-scale vortex tube is performed. Because of the small size of nozzles, it is essential to check the validation of continuum model in the micro-scale vortex tube. The continuum model is not valid, when the characteristic dimension is comparable to the mean free path of the molecules. The ratio of the mean free path to the characteristic length, defines an important dimensionless parameter, called the Knudsen number, and it is given by [24, 27]:

$$Kn = \sqrt{\frac{\pi\gamma}{2}}\frac{M_{in}}{Re_{in}}, \quad \text{where} \quad Re = \frac{\dot{m}d_n}{4A\mu} \tag{1}$$

For the values of $Kn \leq 0.001$, the flow-regime is continuum. At the inlet nozzles, the Knudsen number is equal to $Kn = 8.96 \cdot 10^{-5}$, so it is possible to apply the Navier-Stokes and energy equations in the flow simulation. Furthermore, the velocity and the temperature of the fluid at the boundary is the same as those of the wall.

The flow regime in a vortex tube is mainly classified into two parts: near-wall and central regions. The flow in the central region has a higher level of turbulence and mixing, so using of *k-ε* turbulence model is preferred. On the other hand, due to the viscosity effect, the

622

Rahbar, N., *et al.*: Numerical Investigation on Flow Behavior and Energy …
THERMAL SCIENCE, Year 2015, Vol. 19, No. 2, pp. 619-630

flow near the walls has low velocity with lower value of turbulence, so k-ω turbulence model is the best choice for the numerical simulation of the flow field near the walls. The shear-stress transport *SST k-ω* model, developed by Menter [28], effectively and accurately combines the formulation of k-ω and k-ε turbulence models by using a blending function. The blending function activates k-ω model near the wall, and k-ε model in the central region of the vortex tube. This modification improves the prediction of the flow with strong adverse pressure gradients and separation [29, 30].

In this study, the flow is assumed as steady, turbulent, compressible and the governing equations for fluid flow and heat transfer are:

– continuity equation

$$\frac{\partial}{\partial x_i}(\rho u_i) = 0 \tag{2}$$

– momentum equation

$$\frac{\partial}{\partial x_j}(\rho u_i u_j) = -\frac{\partial P}{\partial x_i} + \frac{\partial}{\partial x_j}\left[\mu\left(\frac{\partial u_i}{\partial x_j} + \frac{\partial u_j}{\partial x_i} - \frac{2}{3}\delta_{ij}\frac{\partial u_k}{\partial x_k}\right)\right] + \frac{\partial u_i}{\partial x_j}\left(-\overline{\rho u_i' u_j'}\right) \tag{3}$$

– energy equation

$$\frac{\partial}{\partial x_i}\left[\rho u_i\left(h + \frac{1}{2}u_i u_j\right)\right] = \frac{\partial}{\partial x_j}\left[k_{\text{eff}}\frac{\partial T}{\partial x_j} + u_i(\tau_{ij})_{\text{eff}}\right], \quad k_{\text{eff}} = K + \frac{c_p \mu_t}{\text{Pr}_t} \tag{4}$$

State equation for an ideal gas is:

$$P = \rho \text{R} T \tag{5}$$

The term of $-\overline{\rho u_i' u_j'}$ is called the Reynolds stress and must be modeled to close the eq. (3). Boussinesq hypothesis is a common method for modeling the Reynolds stresses, and it is given as:

$$-\overline{\rho u_i' u_j'} = \mu_t\left(\frac{\partial u_i}{\partial x_j} + \frac{\partial u_j}{\partial x_i}\right) - \frac{2}{3}\left(\rho k + \mu_t \frac{\partial u_k}{\partial x_k}\right)\delta_{ij} \tag{6}$$

$$\tau_{\text{eff}} = \mu_{\text{eff}}\left(\frac{\partial u_j}{\partial x_i} + \frac{\partial u_i}{\partial x_j}\right) - \frac{2}{3}\mu_{\text{eff}}\frac{\partial u_k}{\partial x_k}\delta_{ij} \tag{7}$$

$$\mu_{\text{eff}} = \mu_t + \mu$$

Using *SST k-ω* model, ω and k satisfy the equations:

$$\frac{\partial}{\partial x_j}(\rho k u_i) = \frac{\partial}{\partial x_j}\left[\Gamma_k\left(\frac{\partial k}{\partial x_j}\right)\right] + \bar{G}_k - Y_k + S_k \tag{8}$$

$$\frac{\partial}{\partial x_j}(\rho \omega u_i) = \frac{\partial}{\partial x_j}\left[\Gamma_\omega\left(\frac{\partial k}{\partial x_j}\right)\right] + G_\omega + D_\omega - Y_\omega + S_\omega \tag{9}$$

More details about the terms of μ_t, Γ_k, S_k, $\bar{G}_k$, Γ_ω, G_ω, D_ω, Y_ω, and S_ω can be found in [29-31].

Rahbar, N., *et al.*: Numerical Investigation on Flow Behavior and Energy …
THERMAL SCIENCE, Year 2015, Vol. 19, No. 2, pp. 619-630

623

Theoretical background

In order to evaluate the performance of a micro-scale vortex-tube, some operational parameters should be calculated as:

– total temperature difference

$$\Delta T_{hc} = T_h - T_c \tag{10}$$

– cold air temperature difference

$$\Delta T_c = T_{in} - T_c \tag{11}$$

– non-dimensional cold air temperature

$$T_c^* = \frac{\Delta T_c}{T_{in}} \tag{12}$$

– refrigeration capacity

$$\dot{Q}_c = \dot{m}_c C_p \Delta T_c \tag{13}$$

– isentropic efficiency

$$\eta_{is} = \frac{\Delta T_c}{\Delta T_{cs}} \tag{14}$$

– isentropic temperature difference [32, 33]

$$\Delta T_{cs} = T_{in} - T_{cs} = T_{in}\left[1 - \left(\frac{P_{atm}}{P_{in}}\right)^{(\gamma-1)/\gamma}\right] \tag{15}$$

– cold mass ratio

$$y_c = \frac{\dot{m}_c}{\dot{m}_{in}} \tag{16}$$

Solution procedures

As shown in figs. 1 and 2, to investigate the flow structure and energy separation phenomena, two types of the micro-scale vortex tube, a 3-D and an axisymmetric 2-D one, were simulated by using Fluent 6.3.26 software.

The 3-D model has four inlet nozzles with 0.382×0.164 mm^2 cross-sectional area. However, in 2-D one, the inlet is modeled as a continuous annular opening with a cross-sectional area equals to the total area of four inlet nozzles. Moreover, the diameter of the cold outlet has been chosen so that its area is the same as the cold-outlet area in 3-D modeling. Table 1 shows the other dimensions of both 3-D and 2-D geometries. In addition, in 3-D modeling, the conic-valve at the hot end is simulated as a radial outlet.

In this study, the experimental results reported by Hamoudi *et al.* [26] are used as boundary conditions. The boundary conditions are:
– mass flow inlet ($\dot{m} = 3.5 \cdot 10^{-5}$ kg/s for each nozzle), total temperature (T_{in} = 296.3 K), turbulence intensity = 5% and turbulence viscosity ratio = 10, were used at the inlets; moreover, in 2-D modeling, the angle between radial velocity component and resultant velocity is considered as 16.62°,
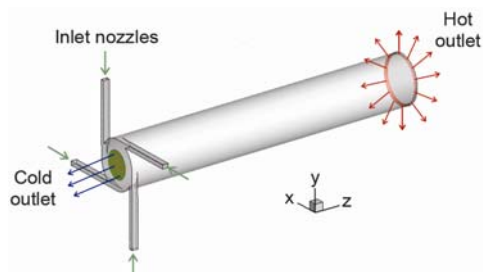
624

Rahbar, N., *et al.*: Numerical Investigation on Flow Behavior and Energy …
THERMAL SCIENCE, Year 2015, Vol. 19, No. 2, pp. 619-630

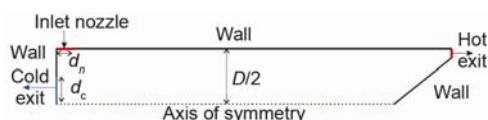**Figure 1. Geometry of the micro-scale vortex tube used in 3-D simulation**

Figure 2. Geometry of the micro-scale vortex tube used in 2-D simulation

Table 1. Dimensions of the micro-scale vortex tubes used for CFD modeling

	L [mm]	D [mm]	d_c [mm]	d_n [mm]
3-D simulation	20	2	1.1	-
2-D simulation	20	2	0.55	0.141

- pressure-outlet boundary conditions with backflow turbulent kinetic energy of 1 m^2/s^2, backflow specific dissipation rate of 1 1/s, and backflow total temperature of 300 K were used for both hot and cold outlets; for cold-outlet its value was equal to atmospheric pressure and, for hot-outlet its value was varied to control the hot-outlet mass fraction [14, 22], and
- adiabatic and no-slip boundary conditions were considered at the walls.

In Fluent 6.3.26, the governing equations of fluid flow are solved by the finite-volume method. For the convection-diffusion formulation, PRESTO was used as a pressure interpolation scheme and second-order upwind was used for others. The pressure-velocity coupling was also handled by using the SIMPLE algorithm, described by Patankar [34, 35]. The air is also considered as an ideal gas with constant specific heat and variable viscosity and thermal conductivity. The solution is considered to be fully converged when the values of the scaled-residuals from iteration to iteration are smaller than a prescribed value 10^{-7} for the energy equation and 10^{-5} for others.

Grid dependency tests have been done for all configurations investigated. The grid independency is attained when the percent changes of total temperature difference and tangential velocity are smaller than a given accuracy value 1%. Total numbers of nodal point for 2-D and 3-D modeling are 14675 and 146500, respectively. Figures 3 and 4 show the grid-dependency plots for the 2-D and the 3-D micro-scale vortex tubes, while fig. 5 shows the typical grids used for the CFD simulations.
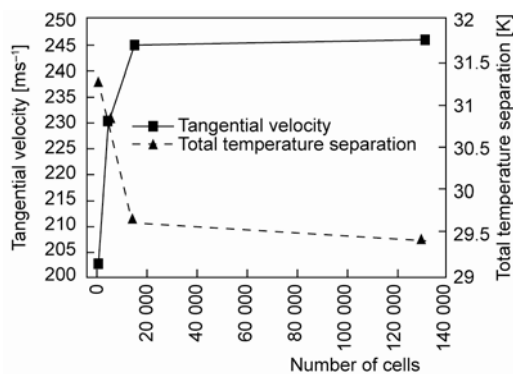

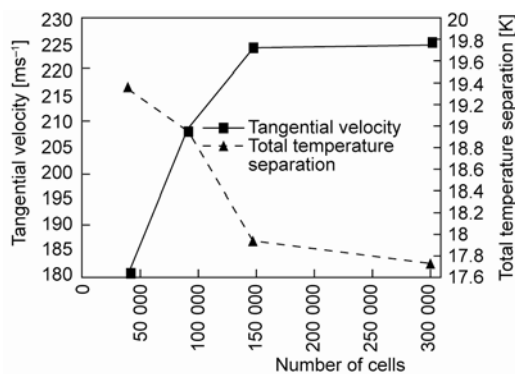**Figure 3. Grid dependency check for a 2-D micro-scale vortex tube**

Figure 4. Grid dependency check for a 3-D micro-scale vortex tube

Rahbar, N., *et al.*: Numerical Investigation on Flow Behavior and Energy …
THERMAL SCIENCE, Year 2015, Vol. 19, No. 2, pp. 619-630

625

Table 2. Maximum deviations from experimental results for 2-D and 3-D CFD simulations

Simulation methods	T_c^*	η_{is}	Q_c	$y_{c,optimum}\big|_{Q_c=Q_{max}}$
3-D simulation	20%	16.6%	12.5%	7%
2-D simulation	84%	84.5%	97%	3%

Figure 5. Typical 3-D grid (top), and typical 2-D grid (bottom)

In order to validate the numerical modeling, the results of CFD-simulations have been compared with the experimental results, reported by Hamoudi *et al.* [26]. The results of comparison are shown in figs. 6-8. On the other hand, the maximum deviations from the experimental-results for 2-D and 3-D simulations are shown in tab. 2. The results indicated that, both numerical and experimental methods have a very good agreement in the prediction of optimum cold mass-ratio y_c. However, the prediction of 3-D simulation is generally more accurate than 2-D one. The results also imply that 3-D CFD simulation has a very good prediction in the lower ranges of cold mass-ratios.

Figure 6. Variation of non-dimensional cold air temperature, numerical and experimental results

Figure 6 also shows that the maximum value for T_c^* is achieved at $y_c = 0.58$, which is the point of maximum-efficiency according to fig. 7. However, as shown in fig. 8, the maximum refrigeration power is obtained when the cold mass-ratio is equal to $y_c = 0.65$. These results are in accordance with the experimental results of commercial vortex-tubes, reported by Skye *et al.* [16].
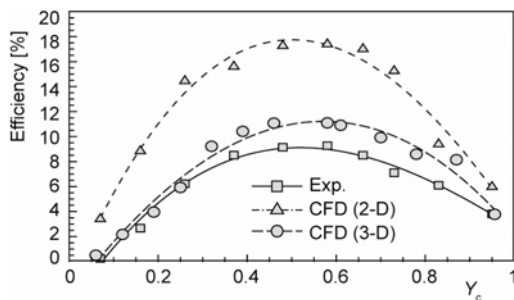
Figure 7. Variation of isentropic efficiency, comparison between numerical and experimental results
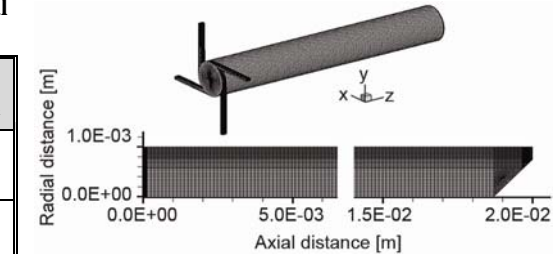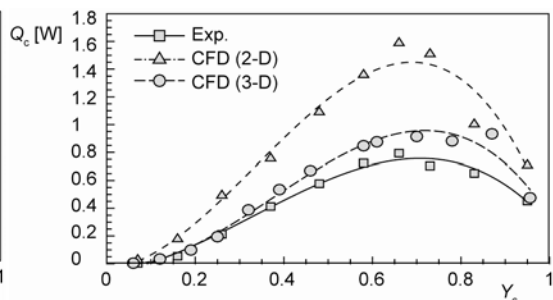
Figure 8. Variation of refrigeration capacity, comparison between numerical and experimental results

Results and discussions

To study the flow field in the micro-scale vortex tube, the results of a 3-D CFD-simulation for the case of $P_{in} = 200$ kPa, and $y_c = 0.58$, in which the optimum T_c^* is occurred,

626

Rahbar, N., *et al.*: Numerical Investigation on Flow Behavior and Energy …
THERMAL SCIENCE, Year 2015, Vol. 19, No. 2, pp. 619-630

have been used. The variation of tangential velocity along radial-direction for different cross-sections of the micro-scale vortex tube is shown in fig. 9. It is concluded that the tangential velocity near the inlet-zone is greater than those of the other zones. This is because of decreasing in the tangential velocity alongside the vortex tube as a result of wall friction and friction between the fluid-layers. Moreover, due to the existence of a forced-vortex in most central parts of the tube, the tangential velocity linearly increases to its maximum value at $r \approx 0.8\ R$. After that it rapidly decreases to zero. This is because of the presence of a free vortex zone due to the viscous boundary layer near the wall [36].

The variation of axial velocity along the radial direction is shown in fig. 10. The axial velocity is zero near $r = 0.75\ R$, which is the separating-line between hot and cold streams. For the values of $r > 0.75\ R$, the direction of flow is toward the hot-outlet, and for the values of $r < 0.75\ R$, its direction is toward the cold-outlet.
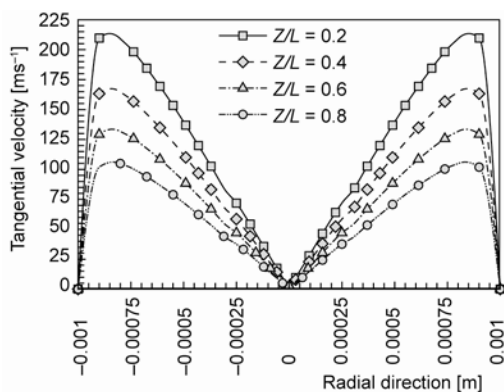

Figure 9. Variation of tangential velocity in radial direction; $P_{in} = 200$ kPa, $y_c = 0.58$
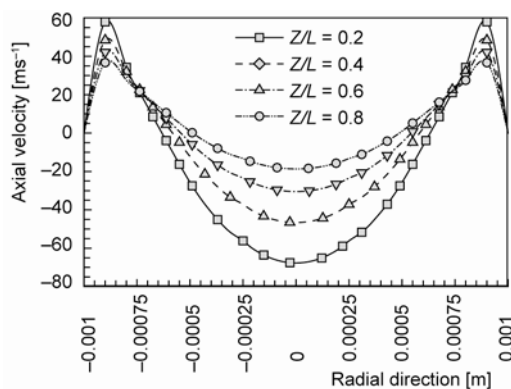
Figure 10. Variation of axial velocity in radial direction at different cross-sections; $P_{in} = 200$ kPa, $y_c = 0.58$

The temperature separation was happened because of some parameters. It was reported that the sudden expansion in the entrance region and the compression of air at the peripheral zone, are the main reasons for the temperature separation in a vortex tubes. The static pressure distribution along the radial direction for different cross-sections of the tube was shown in fig. 11. The results show that for the values of $r < 0.75\ R$, the static pressure increases by moving from inlet nozzles toward the hot-outlet. This means that there exists a flowing stream from hot-outlet to cold-outlet in the central part of the tube. However, for the values of $r > 0.75\ R$, the static pressure decreases along the axial direction and so, the direction of flow is toward the hot-outlet. Moreover, the static pressure was constant on the separating-line between hot and cold streams. The streamlines, for peripheral and central zones of the micro-scale vortex tube, are shown in figs. 12 and 13.
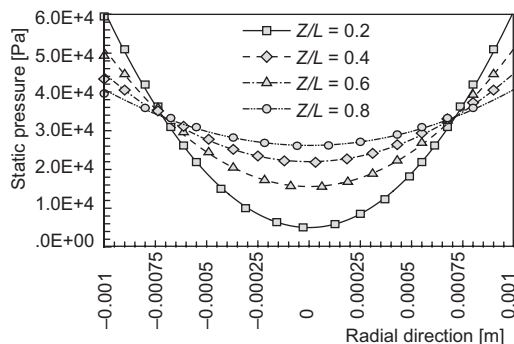
The static temperature gradient may be another reason for the temperature separation phenomenon. Figure 14 shows the tempera-
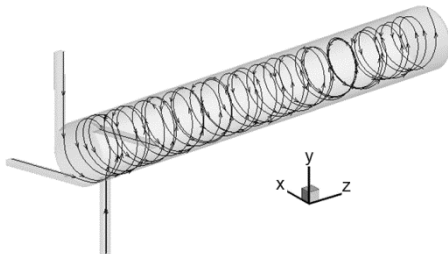

Figure 11. Variation of static pressure in radial direction at different cross-sections; $P_{in} = 200$ kPa, $y_c = 0.58$

Rahbar, N., *et al.*: Numerical Investigation on Flow Behavior and Energy …
THERMAL SCIENCE, Year 2015, Vol. 19, No. 2, pp. 619-630

627

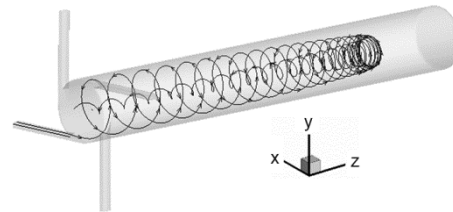**Figure 12. Streamline for a fluid element in peripheral region (hot-stream)**

Figure 13. Streamline for a fluid element in central region (cold-stream)

ture distribution as a function of radius, along the micro-scale vortex tube. It is seen that, in the core-zone of the tube, the static temperature rapidly decreases from the hot-outlet toward the cold-outlet. However, it slightly increases in the peripheral zone of the micro-scale vortex tube. Behera *et al.* [36] reported that, in a large-scale vortex tube, the static temperature radially decreases near the entrance region. Figure 14 shows that this phenomenon is also happened in a micro-scale vortex tube as a result of flow expansion after leaving of inlet nozzles. Moreover, it is seen that, except near the entrance zone, the static temperature is radially constant in the core-zone of the micro-scale vortex tube. The variation of total velocity as a function of radius is shown in fig. 15. It can be concluded that, the velocity magnitude rapidly varies in the radial direction unlike the static temperature distribution. This means that the temperature-separation in the micro-scale vortex tube is a function of the variation of kinetic energy, and the expansion of air in the radial direction.
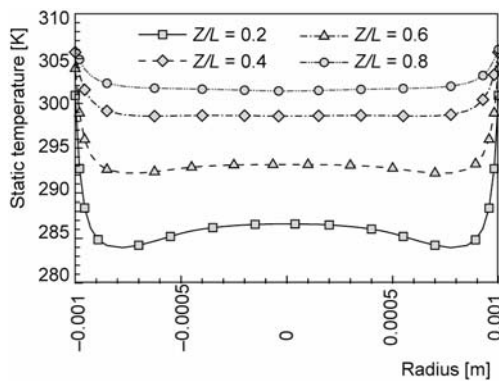

Figure 14. Variation of static temperature in radial direction at different cross-sections; $P_{in} = 200$ kPa, $y_c = 0.58$
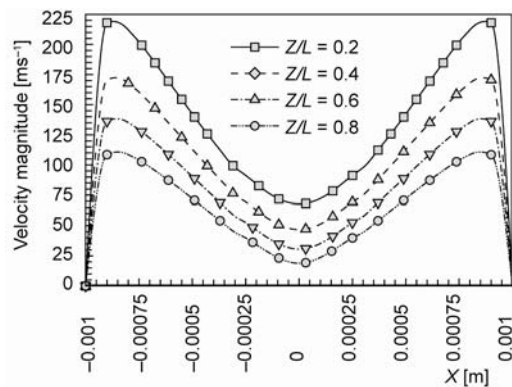
Figure 15. Variation of velocity magnitude in radial direction at different cross-sections; $P_{in} = 200$ kPa, $y_c = 0.58$

The effects of tube-length on isentropic efficiency and refrigeration capacity are shown in figs. 16 and 17. Conclusion is that in a fixed cold-mass ratio, the effect of tube-length increases when y_c approaches to the optimum value of cold-mass ratio. On the other hand, the refrigeration capacity is approximately independent of tube-length for the values of cold-mass ratio smaller than $y < 0.35$. Contours of static temperature of a micro-scale vortex tube are in fig. 18. The results show that minimum temperature is happened where the flow leaves the inlet-nozzles. Figure 19 shows the total temperature distribution for the length of $L = 20$ mm of a micro-scale vortex tube. It is seen that peripheral flow is warm and core flow is cold.
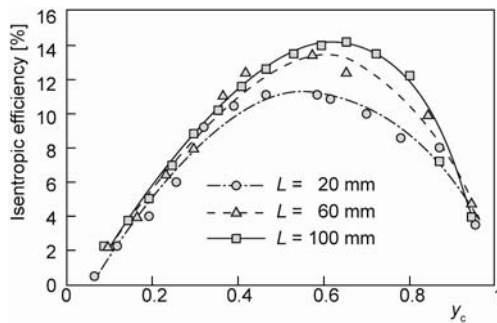
628

Rahbar, N., *et al.*: Numerical Investigation on Flow Behavior and Energy …
THERMAL SCIENCE, Year 2015, Vol. 19, No. 2, pp. 619-630

Figure 16. The effect of tube-length on the isentropic efficiency of micro-scale vortex tubes; P_{in} = 200 kPa, d_c = 1.1 mm
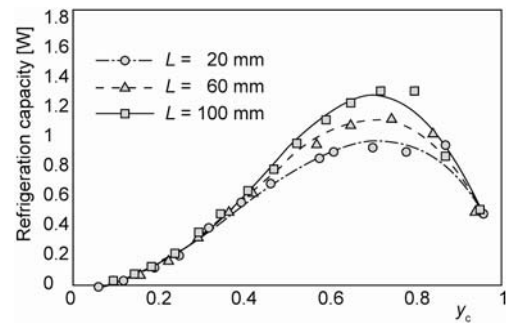
Figure 17. The effect of tube-length on the refrigeration capacity of micro-scale vortex tubes; P_{in} = 200 kPa, d_c = 1.1 mm
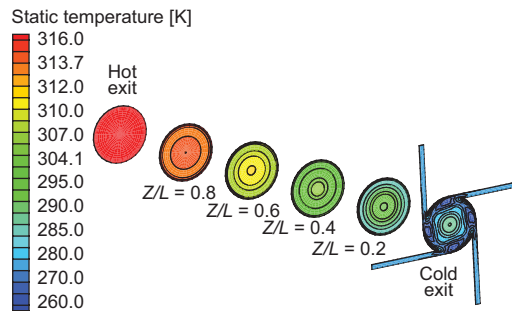
Figure 18. Contours of static temperature at Z/L = 0.2, Z/L = 0.4, Z/L = 0.6, and Z/L = 0.8; P_{in} = 200 kPa, y_c = 0.58, L = 20 mm
(for color image see journal web-site)

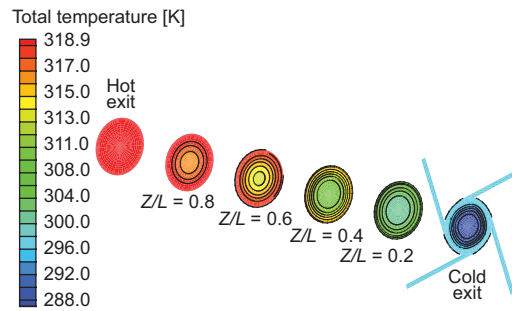**Figure 19. Contours of total temperature at Z/L = 0.2, Z/L = 0.4, Z/L = 0.6, and Z/L = 0.8;** P_{in} = 200 kPa, y_c = 0.58, L = 20 mm
(for color image see journal web-site)

Conclusions

In this study, the energy separation in a micro-scale vortex tube was investigated by using of the computational fluid dynamic. For this purpose, a 2-D and a 3-D model have been simulated by Fluent 6.3.26 software, and their results have been compared with the experimental results reported in the literature. The main results obtained may be summarized.

- Both numerical simulations have a good agreement with experimental results. However, the 3-D CFD simulation is more accurate than 2-D one.
- The maximum T_c^* and the maximum efficiency are happened at y_c = 0.58.
- The maximum refrigeration power is achieved at y_c = 0.65.
- The tangential velocity near the inlet-zone is greater than the other zones. This is because of decreasing of the tangential velocity alongside the vortex tube as a result of wall friction and friction between the fluid-layers.
- The value of r = 0.75 R is the separating-line between hot and cold streams.
- Unlike large-scale vortex tubes, the static temperature radially increases near the entrance of the micro-scale vortex tube, which means that, in this region, the expansion-effect on the static temperature is more than that of the large-scale vortex tubes.
- Results of static temperature, velocity magnitude and pressure distributions show that the temperature-separation in the micro-scale vortex tube is a function of the variation of kinetic energy, and the expansion of air in the radial direction.

Rahbar, N., *et al.*: Numerical Investigation on Flow Behavior and Energy …
THERMAL SCIENCE, Year 2015, Vol. 19, No. 2, pp. 619-630

629

- In a fixed cold-mass ratio, the effect of tube-length increases when y_c approaches to the optimum value of cold-mass ratio.
- The refrigeration capacity is approximately independent of tube-length for the values of cold-mass ratio smaller than $y < 0.35$.

Acknowledgment

Nomenclature

A – area, [m^2]
c_p – specific heat at constant pressure, [Jkg^{-1}K^{-1}]
D, d_n – diameter, [m]
h – mass average enthalpy, [Jkg^{-1}]
K – thermal conductivity, [Wm^{-1}K^{-1}]
Kn – Knudsen number, [–]
k – turbulence kinetic energy, [m^{2}s^{-2}]
L – length, [m]
M – Mach number, [–]
$\dot{m}$ – mass flow rate, [kgs^{-1}]
P – pressure, [Pa]
Pr – Prandtl number, [–]
$\dot{Q}_c$ – refrigeration capacity, [W]
R – specific constant of an ideal gas, [Jkg^{-1}K^{-1}]
Re – Reynolds number, [–]
T – temperature, [K]
u – mass averaged velocity, [ms^{-1}]
u' – fluctuating velocity component, [ms^{-1}]
y_c – cold mass fraction, [–]

Greek symbols

γ – specific heat ratio, (c_p/c_v), [–]
δ_{ij} – Kronecker delta
η_{is} – isentropic efficiency
μ – viscosity, [Nsm^{-2}]
μ_t – eddy viscosity, [Nsm^{-2}]
ρ – density, [kgm^{-3}]
τ – stress tensor
ω – specific dissipation rate

Subscripts

in – inlet
c – cold
h – hot
is – isentropic
hc – hot-cold
atm – atmospheric

References

[1] Ranque, G., Experiments on Expansion in a Vortex with Simultaneous Exhaust of Hot Air and Cold Air, *Le Journal de Physique et le Radium,4* (1933), 6, pp. 112-114
[2] Ranque, G., Method and Apparatus for Obtaining from a Fluid under Pressure Two Outputs of Fluid at Different Temperatures, US Patent 1:952, 281, 1934
[3] Hilsch, R., The Use of the Expansion of Gases in a Centrifugal Field as Cooling Process, *Review of Scientific Instruments,18* (1947), 2, pp. 108-113
[4] Eiamsa-Ard, S., Promvonge, P., Numerical Simulation of Flow Field and Temperature Separation in a Vortex Tube, *International Communications in Heat and Mass Transfer, 35* (2008), 8, pp. 937-947
[5] Saidi, M. Valipour, M., Experimental Modeling of Vortex Tube Refrigerator, *Applied Thermal Engineering, 23* (2003), 15, pp. 1971-1980
[6] Gao, C., *et al.*, Experimental Study on a Simple Ranque-Hilsch Vortex Tube, *Cryogenics, 45* (2005), 3, pp. 173-183
[7] Aydin, O., Baki, M., An Experimental Study on the Design Parameters of a Counterflow Vortex Tube, *Energy, 31* (2006), 14, pp. 2763-2772
[8] Hamdan, M., *et al.*, Experimental Analysis on Vortex Tube Energy Separation Performance, *Heat and Mass Transfer, 47* (2011), 12, pp. 1637-1642
[9] Wu, Y. T., *et al.*, Modification and Experimental Research on Vortex Tube, *International Journal of Refrigeration, 30* (2007), 6, pp. 1042-1049
[10] Nimbalkar, S. U., Muller, M. R., An Experimental Investigation of the Optimum Geometry for the Cold End Orifice of a Vortex Tube, *Applied Thermal Engineering, 29* (2009), 2-3, pp. 509-514

[11] Valipour, M. S., Niazi, N., Experimental Modeling of a Curved Ranque-Hilsch Vortex Tube Refrigerator, *International Journal of Refrigeration, 34* (2011), 4, pp. 1109-1116

[12] Frohlingsdorf, W., Unger, H., Numerical Investigations of the Compressible Flow and the Energy Separation in the Ranque-Hilsch Vortex Tube, *Int. Journal of Heat and Mass Transfer, 42* (1999), 3, pp. 415-422

[13] Keyes Jr, J., An Experimental Study of Gas Dynamics in High Velocity Vortex Flow, *Proceedings,* Heat Transfer and Fluid Mechanics Institute, Stanford University, Oak Ridge National Laboraty, Tenn., USA, 1960, pp. 31-46

[14] Behera, U., *et al.*, CFD Analysis and Experimental Investigations towards Optimizing the Parameters of Ranque-Hilsch Vortex Tube, *Int. Journal of Heat and Mass Transfer, 48* (2005), 10, pp. 1961-1973

[15] Aljuwayhel, N. F., *et al.*, Parametric and Internal Study of the Vortex Tube Using a CFD Model, *International Journal of Refrigeration, 28* (2005), 3, pp. 442-450

[16] Skye, H. M., *et al.*, Comparison of CFD Analysis to Empirical Data in a Commercial Vortex Tube, *International Journal of Refrigeration, 29* (2006), 1, pp. 71-80

[17] Eiamsa-ard, S., Promvonge, P., Numerical Investigation of the Thermal Separation in a Ranque-Hilsch Vortex Tube, *International Journal of Heat and Mass Transfer, 50* (2007), 5-6, pp. 821-832

[18] Ameri, M., Behnia, B., The Study of Key Design Parameters Effects on the Vortex Tube Performance, *Int. Journal of Thermal Science, 18* (2009), 4, pp. 370-376

[19] Farouk, T., Farouk, B., Large Eddy Simulations of the Flow Field and Temperature Separation in the Ranque-Hilsch Vortex Tube, *Int. Journal of Heat and Mass Transfer, 50* (2007), 23-24, pp. 4724-4735

[20] Farouk, T., *et al.*, Simulation of Gas Species and Temperature Separation in the Counter-Flow Ranque-Hilsch Vortex Tube Using the Large Eddy Simulation Technique, *Int. Journal of Heat and Mass Transfer, 52* (2009), 13-14, pp. 3320-3333

[21] Hossein-Nezhad, A. Shamsoddini, R., Numerical Three-Dimensional Analysis of the Mechanism of Flow and Heat Transfer in a Vortex Tube, *Thermal Science, 13* (2009), 4, pp. 183-196

[22] Shamsoddini, R. Hossein-Nezhad, A., Numerical Analysis of the Effects of Nozzles Number on the Flow and Power of Cooling of a Vortex Tube, *International Journal of Refrigeration, 33* (2010), 4, pp. 774-782

[23] Dutta, T., *et al.*, Comparison of Different Turbulence Models in Predicting the Temperature Separation in a Ranque-Hilsch Vortex Tube, *International Journal of Refrigeration, 33* (2010), 4, pp. 783-792

[24] Hamoudi, A. F., An Investigation of a Micro-Scale Ranque-Hilsch Vortex Tube, M. Sc. thesis, Mechanical, Automotive and Materials Engineering Department, University of Windsor, Windsor, Ont., Canada, 2006

[25] Dyskin, L., Kramarenko, P., Energy Characteristics of Vortex Microtubes, *Journal of Engineering Physics and Thermophysics, 47* (1984), 6, pp. 1394-1395

[26] Hamoudi, A., *et al.*, Performance Characteristics of a Microscale Ranque-Hilsch Vortex Tube, *Journal of Fluids Engineering, 130* (2008), 10, 101206

[27] Zhang, Z., *Nano/Microscale Heat Transfer*, McGraw-Hill Professional, 1st ed., 2007

[28] Menter, F. R., Two-Equation Eddy-Viscosity Turbulence Models for Engineering Applications, *AIAA Journal, 32* (1994), 8, pp. 1598-1605

[29] Cebeci, T., *Analysis of Turbulent Flows,* 2nd ed., Elsevier, San Diego, Cal., USA, 2004

[30] Cebeci, T., *Turbulence Models and Their Application: Efficient Numerical Methods with Computer Programs,* Horizons Pub. and Springer, New York, Berlin, 2004

[31] ***, FLUENT 6.3 User's Guide, Fluent Inc., 2006

[32] Xue, Y., *et al.*, A Critical Review of Temperature Separation in a Vortex Tube, *Experimental Thermal and Fluid Science, 34* (2010), 8, pp. 1367-1374

[33] Yilmaz, M., *et al.*, A Review on Design Criteria for Vortex Tubes, *Waerme- und Stoffuebertragung, 45* (2009), 5, pp. 613-632

[34] Patankar, S. V., *Numerical Heat Transfer and Fluid Flow*, Hemisphere Pub., New York, USA, 1980

[35] Versteeg, H. K. Malalasekera, W., *An Introduction to Computational Fluid Dynamics: the Finite Volume Method*, Prentice Hall, Harlow, UK, 2007

[36] Behera, U., *et al.*, Numerical Investigations on Flow Behavior and Energy Separation in Ranque-Hilsch Vortex Tube, *International Journal of Heat and Mass Transfer, 51* (2008), 25-26, pp. 6077-6089